Accepted Manuscript

Reduced deuterium retention in simultaneously damaged and annealed tungsten

M.J. Simmonds, Y.Q. Wang, J.L. Barton, M.J. Baldwin, J.H. Yu, R.P. Doerner, G.R. Tynan

PII: S0022-3115(17)30024-7

DOI: 10.1016/j.jnucmat.2017.06.010

Reference: NUMA 50344

To appear in: *Journal of Nuclear Materials*

Received Date: 5 January 2017

Revised Date: 2 June 2017

Accepted Date: 6 June 2017

Please cite this article as: M.J. Simmonds, Y.Q. Wang, J.L. Barton, M.J. Baldwin, J.H. Yu, R.P. Doerner, G.R. Tynan, Reduced deuterium retention in simultaneously damaged and annealed tungsten, *Journal of Nuclear Materials* (2017), doi: 10.1016/j.jnucmat.2017.06.010.

Reduced Deuterium Retention in Simultaneously Damaged and Annealed Tungsten

M.J. Simmonds [1a], Y.Q. Wang[b], J.L. Barton[c], M.J. Baldwin[a], J.H. Yu[a], R.P. Doerner[a], G.R. Tynan[a,d]

[a] *Center for Energy Research, UC San Diego, 9500 Gilman Dr., La Jolla, CA 92093-0417, USA*
[b] *Materials Science and Technology Division, Los Alamos National Laboratory, Los Alamos, NM 87545, USA*
[c] *Sandia National Laboratories, Energy Innovation Department, Livermore, CA 94550, USA*
[d] *Department of Mechanical and Aerospace Engineering (MAE), UC San Diego, 9500 Gilman Dr., La Jolla, CA 92093-0411, USA*

Abstract

Deuterium (D) retention in polycrystalline tungsten (W) with copper (Cu) ion damage concurrently produced at elevated surface temperature is investigated. An in situ heated stage held W samples at a controlled temperature up to 1243 K, which were subjected to displacement damage produced by 3.4 MeV Cu ions. D retention is subsequently explored by exposure of the W samples held at 383 K to a D_2 plasma ion fluence of 10^{24} D^+/m^2. Nuclear reaction analysis (NRA), utilizing the $D(^3He,p)^4He$ nuclear reaction, is used to probe the D concentration in the near surface up to 6 μm. Thermal desorption spectroscopy (TDS) is used to measure outgassed HD and D_2 molecules to determine the bulk D concentration. Both NRA and TDS measure a significant reduction in D retention for samples damaged at elevated temperature. TDS quantitatively shows that the lowest energy trap remains largely unaffected while higher energy traps, induced by Cu ions, are annealed and approach intrinsic concentrations as the temperature during ion damage approaches 1243 K. Analysis of TDS data yields an activation energy of (0.10 $\pm$ 0.02) eV for recovery of ion-damage induced traps at elevated temperature.

Keywords: Tungsten, Dynamic Annealing, Deuterium, Retention, Recovery, Concurrent Ion Beam Damage, NRA, TDS

Email address: msimmonds@eng.ucsd.edu (M.J. Simmonds)

1. Introduction

The trapping and retention of tritium fuel within neutron damaged plasma facing components (PFC) is of primary concern for next step fusion devices such as ITER and DEMO [1]. However, the direct study of neutron damaged material is difficult due to the time needed for activated samples to decay back to safe levels and the lack of high flux neutron sources to produce a fusion relevant fluence in a short period of time [2]. As such, the use of heavy ion damage and deuterium as a proxy for neutrons and tritium, respectively, allow for more timely experimental studies of fundamental aspects of this important problem. The reader is referred to ASTM E521 [3] for the key differences between neutron and heavy ion displacement damage.

Currently, W is the primary PFC candidate for first wall and divertor armor due to its high melting point, low H isotope retention, and resistance to sputtering [1]. Relevant PFC temperatures span 373 to 1273 K for tokamak devices such as ITER and DEMO [4]. Previous studies that induced ion damage near room temperature followed by subsequent annealing steps before or during plasma exposure have shown a reduction in D retention [5, 6]. In order to further isolate and investigate fusion relevant damage production and recovery, heavy ion damage was performed while simultaneously heating/annealing W samples. In accordance with similar experiments [7, 8], the concurrent heavy ion irradiation at elevated temperature will be referred to as dynamic annealing. In this experiment, further recovery of defects during plasma exposure is limited by holding the sample at a low temperature of 383 K. This sample temperature still allows rapid D diffusion in W [9] while limiting the release rate, thus allowing D to occupy near-surface ion induced traps. These considerations allow D to act as an effective marker for trap sites that can be probed by NRA and TDS techniques.

2. Experiment

2.1. W Sample Preparation

Supplied by Midwest Tungsten, samples were cut from certified 99.95 wt.% powder metallurgy polycrystalline W rod, 6 mm in diameter and 1.5 mm thick. The surfaces to be exposed to plasma were mechanically polished down to 3 μm grit, producing a mirror finish. Afterwards, the samples were cleaned in ultrasonic baths, first in acetone and then ethanol. To further relieve mechanical stress and reduce intrinsic defects, the samples were then annealed *in vacuo* below 10^{-4} Pa at 1173 K for 1 hour. Under a scanning electron microscope, an annealed sample broken in half was observed to display elongated grains perpendicular to the surface with dimension on the order of 10 μm parallel to the surface.

2.2. Heavy-ion Displacement Damage in W

In the Ion Beam Materials Laboratory (IBML) at Los Alamos National Laboratory (LANL), a tandem ion accelerator irradiated the polished W samples with 3.4 MeV Cu^{2+} ions. Cu was chosen over W, since the lighter Cu ions penetrate deeper for comparable energies. SRIM-2012 [10] was used to estimate the displacements per atom (dpa) profile as a function of the beam parameters. Per Stoller *et al.* [11], the "Quick" Kinchin-Pease option and a displacement damage threshold of 90 eV for W were used. A peak dpa of 0.2, achieved by a dose of 1.82 x 10^{18} ions/m^2 with an average flux of $\sim 10^{15}$ ions/m^2/s, ensured the implanted Cu remained below intrinsic Cu impurity levels [12].

In general, the ion beam community follows the practice recommended by ASTM [3] when performing ion irradiations. Specifically, it recommends to use a defocussed ion beam to avoid periodic local flux variations artificially introduced when rastering a beam. However, it is also a common challenge to produce a uniform irradiated sample with the defocussed beam. We chose the rastering beam to produce a relatively large damaged sample size with excellent lateral uniformity.

2.3. Concurrent Heating During Damage

A vacuum chamber at IBML with a heated stage was used to hold W samples at 300, 573, 873, 1023, or 1243 K during Cu ion irradiation, inducing dynamic annealing. The samples were affixed to a Ni slab that housed heating elements as well as a thermocouple used to measure the sample temperature. Before Cu ion implantation, the sample holder was heated to the desired plateau temperature. To ensure damage uniformity, the ion implantation was then performed by raster scanning across an area larger than the sample. Prior to reaching the sample, the ion beam was masked to allow the center of the scan to reach the sample while indirectly measuring the current by four corner positioned Faraday cups. Once the desired Cu ion dose was reached, the beam and heating elements were shut off. The sample holder was then actively cooled with pressurized air to decrease the temperature by half the plateau/room temperature difference within a minute, limiting additional post irradiation annealing of defects.

2.4. D_2 Plasma Exposure

One undamaged sample, as well as the Cu ion irradiated samples, were exposed to D_2 plasma with a neutral pressure of $\sim$0.7 Pa at UCSD in the PISCES-E device, a plasma etcher with a 13.56 MHz RF source [13]. An RF compensated Langmuir probe measured a flux of $\sim 10^{20}$ ions/m^2/s uniformly across the surface of the sample holder. The probe was positioned near the sample holder and the voltage was swept as described in Ref. [14]. A total fluence of 10^{24} D/m^2 was chosen to decorate the defects throughout the damage region. During plasma exposure the sample holder was negatively biased to achieve an ion energy of 110 eV and air cooled to 383 K as measured by a thermocouple in contact with the rear of the sample. As noted by Yu [15], the molecular ion concentrations were calculated to be 0.72, 0.06, and 0.22 for D^+, $D_2{}^+$, and $D_3{}^+$ respectively.

2.5. Nuclear Reaction Analysis (NRA)

After the plasma exposure, the D(^{3}He,p)^{4}He nuclear reaction was used to measure depth profiles of D concentration through NRA as prescribed by Mayer [16]. At IBML, a ^{3}He ion

beam was used to probe the D implanted W samples. Increasing ^{3}He energies of 0.6, 0.8, 1.1, 1.5, 2.0, 2.5 and 3.5 MeV probed the first 6 μm. The energy spectrum of protons captured in a solid state detector was used to determine the depth distribution of the nuclear reactions. The 2 mm thick Si detector was protected from elastically scattered ^{3}He and reactant ^{4}He by a 24 μm thick Al foil. Proton counts were binned according to the detector energy resolution of 22 keV. Two software programs were employed to extract D depth profiles. SIMNRA was used to calibrate and simulate the proton energy spectrum produced from a given D depth profile [16, 17]. To fit the proton energy spectra associated with each ^{3}He energy, the software requires the user to input and adjust both a D concentration and associated W layer thickness. NRADC calls upon multiple instances of SIMNRA and utilizes a Markov Chain Monte Carlo scheme to optimize fits for concentration and thickness, producing the most probable D depth profile [18].

2.6. Thermal Desorption Spectroscopy (TDS)

The thermal desorption of D from the samples' surface and total D retention throughout the bulk were measured with TDS. Samples were mounted with a thermocouple pressed against the rear surface, pumped down to a vacuum below 10^{-6} Pa, and heated by infrared lamps at a constant rate of 0.5 K/s before plateauing near 1300 K. D trapped in lattice defects acquires thermal energy to escape, diffuse, trap, and repeat many times before reaching the surface. In order to leave the surface, recombination to form a free molecule must occur. The partial pressures of H_2, HD, and D_2 were measured with a quadrupole mass spectrometer (QMS). A calibrated D_2 leak was used to convert the partial pressure from the QMS to a thermally desorbed particle flux from the sample. The total D flux was calculated as described by Yu [15], as the sum of the HD and twice the D_2 flux. Note that the HD flux was calibrated to the D_2 leak, without any further correction for ionization efficiency, and contributed an average of 25% of the total D flux.

Depending on ambient laboratory humidity, temperature, and the length of vacuum break, the installation of a sample allows water to be adsorbed on the vacuum chamber walls when exposed to atmosphere. These walls were indirectly heated while performing

TDS on a sample, creating H_2, HD, and D_2 signals due to degassing water. The isotopic partial pressure is typically small for HD and D_2 relative to H_2, with a natural abundance below 10^{-3} and 10^{-4} respectively. With increasing temperature this water vapor contribution becomes large enough that it must be corrected. In order to remove this background signal, the dominant H_2 is scaled separately to the HD and D_2 signals. After the initial 0.5 K/s temperature ramp, Figure 2 demonstrates the use of several additional temperature ramps to aid in the linear scaling and offset of H_2 to HD and D_2.

3. Results

NRA depth profiles shown in Figure 1 demonstrate the reduction of D inventory as the dynamic annealing temperature increases. The control sample was not subject to heavy ion damage but displays D agglomeration in the very near surface, below 0.1 μm, due to stress from plasma implantation [19]. The damaged samples trapped a significant inventory of D within the SRIM predicted displacement damage profile. Since all samples were annealed well below the re-crystallization temperature of 1573 K during preparation, intrinsic defects survive and provide trap sites throughout the samples beyond the ion damage zone.

The TDS data in Figure 3 displays multiple D release peaks near 480, 600, and 825 K assigned as peaks 1, 2, and 3 respectively. Peak 1 is present in all samples and is associated with intrinsic defects that survived the annealing during preparation. Peaks 2 and 3 are largest for the sample damaged at 300 K and are significantly lower for the undamaged sample, demonstrating that these peaks are primarily due to ion induced damage. Previously, each peak has been associated with a de-trapping energy modeled as 0.85, 1.45, and 1.85 eV in Ref. [6]. According to that work, peak 1 corresponds to dislocations and grain boundaries, peak 2 to vacancies, and peak 3 to vacancy clusters. Also of note, the initial release of D occurs near 383 K, the sample temperature during D_2 plasma exposure. The total D retention from NRA and TDS measurements are compared in Figure 4. The spatially integrated D profile from NRA accounts for the first 6 μm, while TDS probes the entire sample. Both NRA and TDS monotonically decrease towards the D retained within the control sample.

In order to isolate the recovery of each type of defect, a Gaussian was fit to each release peak. For the case in which desorption peaks overlap, traps become coupled as D atoms escape/trap/migrate through the W lattice. To first order, the sum of Gaussians can reasonably represent thermal desorption as a function of temperature in the case of clearly separated release peaks [20, 21]. Holding the width and position fixed for each individual peak, only the amplitude was varied in the fitting for all samples. The sum of the 3 Gaussians fit to the room temperature damaged sample as well as each individual Gaussian are plotted in Figure 5, demonstrating the well resolved release peaks.

The total D retention for each release peak is plotted in Figure 6 as the integrated area under each Gaussian. The D retention for release peak 1 is relatively constant for all damaged samples as well as the control/undamaged sample. D retention for release peaks 2 and 3 is highest for the room temperature damaged sample. For peaks 2 and 3, increasing the dynamic annealing temperature leads to decreased retention. The sample dynamically annealed at 1243 K approached the level of retention found in the control sample. While NRA displays there is D retained within the displacement zone, the TDS data shows that it is primarily stored in peak 1.

4. Discussion

In experiments similar to this work, Sakurada [7], Ogorodnikova [8], and Markina [21] utilized D retention to study the annealing of heavy ion damaged W samples. Each experiment's specific heavy ion species and energy resulted in a unique dpa profile. By normalizing the total D retention to each respective dpa profile as shown in Figure 7, all five experimental conditions can be directly compared. In order to account for the previously reported saturation of D retention [5], the data from Markina was scaled down to 0.45. A general trend of decreased D retention with increased annealing temperature occurs for both dynamic and post irradiation annealing. In contrast to the other experiments, Ogorodnikova's NRA demonstrated a local increase in total D retention near an annealing temperature of 1000 K for both the dynamic and post annealed samples. By 1300 K, Ogorodnikova observed nearly complete recovery from post irradiation annealing.

Similar to Sakurada, this work prepared samples well below the recrystallization temperature and exposed to a D_2 plasma at a low enough temperature to populate peak 1. TDS for both experiments demonstrated a nearly constant contribution to the total D inventory in peak 1, regardless of annealing temperature.

The TDS profiles for Markina and this work display a monotonic D reduction in peaks 2 and 3. Sakurada observed the same trend for 0.3 and 1.0 dpa damaged samples. However for 0.1 dpa, while peak 3 significantly decreases, peak 2 grows for samples both dynamic and post annealed at 1173 K. Eleveld [22] had previously observed a shift reducing peak 3 and increasing peak 2 occurring above 1040 K. As remarked in Sakurada's paper, the various discrepancies among each work may show the sensitivity of defect recovery to dpa level. That is, the rates of vacancy-cluster and cluster-cluster formation competing with interstitial and free surface annihilation depend on the available concentration of these defects. For instance, the saturation of heavy ion induced defects as dpa approaches 0.3 that has not been observed for neutron damaged W.

To quantify the recovery of heavy ion induced defects at elevated temperatures, we define the fractional recovery of each trap at each dynamic annealing temperature, $F_t(T)$, by subtracting and normalizing the D retention, $R_t(T)$, with respect to the sample damaged at 300 K (i.e. room temperature): $F_t(T) = (R_t(300K) - R_t(T))/R_t(300K)$. The Arrhenius plot, $F_t(T)$ vs. T^{-1}, in Figure 8 demonstrates that heavy ion induced defects associated with peaks 2 and 3 are thermally activated and recover with an activation energy near 0.1 eV.

The relatively low activation energy for this recovery is similar to that reported for self interstitial atom (SIA) mobility [23]. While the recovery of W has been shown to have temperature stages in which various defects become mobile [24], recovery is the sum of these processes. With elevated sample temperature, the probability of the vacancy/SIA pair recombining increases due to the increased mobility of each. Though vacancy mobility has been shown to start near 523 K [25], at 1.7 eV the activation energy is an order of magnitude too large to be the primary source of recovery [26]. Thus the current work is more consistent with SIA mobility as the dominant recovery mechanism since they are

simply the most mobile defect.

Lastly we remark on the recovery of neutron damage at elevated temperatures. One major difference between ion and neutron induced damage is the displacement rate. Typical experiments utilize ion dpa rates that are 10^3 to 10^4 times faster than fusion neutrons are predicted to produce [2]. A slower dpa rate will allow for further recovery of damage as mobile SIA will have more time to perform a random walk and possibly recombine with a vacancy or free surface. Neglecting transmutation, these results show that a significant amount of displacement damage from neutrons may be annealed away provided the wall/divertor armor is held at high enough temperature. That is, an optimal temperature window may be possible that limits the net damage induced defect concentration while preventing the loss of favorable elastic and tensile properties.

5. Summary

Utilizing plasma implanted and diffused D in heavy ion damaged W, we have isolated and examined the effect of dynamic annealing due to elevated temperature concurrent with displacement damage. NRA and TDS measure a significant reduction in D retention for samples damaged at elevated temperature, approaching the retention found in a control sample that is undamaged. TDS demonstrates that higher energy, heavy ion induced traps recover with dynamic annealing while the lowest energy, intrinsic trap remains unaffected. The recovery is found to be thermally activated with an activation energy of 0.1 eV and most likely corresponds to the action of SIA mobility.

6. Acknowledgments

This work was supported by U.S. Department of Energy under DE-FG02-07ER54912 and DE-SC0001999 as well as the University of California Office of Presidential Research Fund under 12-LR-237801.

7. References

[1] C. Skinner, A. Haasz, V. Alimov, N. Bekris, R. Causey, R. Clark, J. Coad, J. Davis, R. Doerner, M. Mayer, A. Pisarev, J. Roth, T. Tanabe, Recent advances on hydrogen retention in iter's plasma-facing materials: Beryllium, carbon. and tungsten, Fusion Science and Technology 54 (2008) 891–945.

[2] M. Shimada, G. Cao, Y. Hatano, T. Oda, Y. Oya, M. Hara, P. Calderoni, The deuterium depth profile in neutron-irradiated tungsten exposed to plasma, Physica Scripta 2011 (2011) 014051.

[3] A. E521, Standard Practice for Neutron Radiation Damage Simulation by Charged-Particle Irradiation (1996). Reapproved 2009.

[4] H. Bolt, V. Barabash, G. Federici, J. Linke, A. Loarte, J. Roth, K. Sato, Plasma facing and high heat flux materials needs for {ITER} and beyond, Journal of Nuclear Materials 307 311, Part 1 (2002) 43 – 52.

[5] M. 't Hoen, M. Mayer, A. Kleyn, H. Schut, P. Z. van Emmichoven, Reduced deuterium retention in self-damaged tungsten exposed to high-flux plasmas at high surface temperatures, Nuclear Fusion 53 (2013) 043003.

[6] O. Ogorodnikova, B. Tyburska, V. Alimov, K. Ertl, The influence of radiation damage on the plasma-induced deuterium retention in self-implanted tungsten, Journal of Nuclear Materials 415 (2011) S661 – S666.

[7] S. Sakurada, K. Yuyama, Y. Uemura, H. Fujita, C. Hu, T. Toyama, N. Yoshida, T. Hinoki, S. Kondo, M. Shimada, D. Buchenauer, T. Chikada, Y. Oya, Annealing effects on deuterium retention behavior in damaged tungsten, Nuclear Materials and Energy 9 (2016) 141 – 144.

[8] O. Ogorodnikova, Y. Gasparyan, V. Efimov, . Ciupiski, J. Grzonka, Annealing of radiation-induced damage in tungsten under and after irradiation with 20 mev self-ions, Journal of Nuclear Materials 451 (2014) 379 – 386.

[9] R. Frauenfelder, Solution and diffusion of hydrogen in tungsten, Journal of Vacuum Science and Technology 6 (1969) 388–397.

[10] J. Ziegler, J. Biersack, U. Littmark, The stopping and range of ions in matter, Pergamon Press (1985).

[11] R. Stoller, M. Toloczko, G. Was, A. Certain, S. Dwaraknath, F. Garner, On the use of {SRIM} for computing radiation damage exposure, Nuclear Instruments and Methods in Physics Research Section B: Beam Interactions with Materials and Atoms 310 (2013) 75 – 80.

[12] J. Barton, Y. Wang, T. Dittmar, R. Doerner, G. Tynan, Deuterium retention in tungsten after heavy ion damage and hydrogen isotope exchange in {PISCES}, Nuclear Instruments and Methods in Physics Research Section B: Beam Interactions with Materials and Atoms 332 (2014) 275 – 279.

[13] G. R. Tynan, A. D. B. III, G. A. Campbell, R. Charatan, A. de Chambrier, G. Gibson, D. J. Hemker, K. Jones, A. Kuthi, C. Lee, T. Shoji, M. Wilcoxson, Characterization of an azimuthally symmetric

helicon wave high density plasma source, Journal of Vacuum Science & Technology A 15 (1997) 2885–2892.

[14] K. J. Taylor, S. Yun, G. R. Tynan, Control of plasma parameters by using noble gas admixtures, Journal of Vacuum Science & Technology A: Vacuum, Surfaces, and Films 22 (2004) 2131–2138.

[15] J. Yu, M. Simmonds, M. Baldwin, R. Doerner, Deuterium desorption from tungsten using laser heating, Nuclear Materials and Energy (In Press) (2016).

[16] M. Mayer, E. Gauthier, K. Sugiyama, U. von Toussaint, Quantitative depth profiling of deuterium up to very large depths, Nuclear Instruments and Methods in Physics Research Section B: Beam Interactions with Materials and Atoms 267 (2009) 506 – 512.

[17] M. Mayer, Simnra, a simulation program for the analysis of nra, rbs and erda, AIP Conference Proceedings 475 (1999) 541–544.

[18] K. Schmid, U. von Toussaint, Statistically sound evaluation of trace element depth profiles by ion beam analysis, Nuclear Instruments and Methods in Physics Research Section B: Beam Interactions with Materials and Atoms 281 (2012) 64 – 71.

[19] O. Ogorodnikova, J. Roth, M. Mayer, Deuterium retention in tungsten in dependence of the surface conditions, Journal of Nuclear Materials 313316 (2003) 469 – 477.

[20] M. Poon, A. Haasz, J. Davis, Modeling deuterium release during thermal desorption of d+ -irradiated tungsten, Journal of Nuclear Materials 374 (2008) 390 – 402.

[21] E. Markina, M. Mayer, A. Manhard, T. Schwarz-Selinger, Recovery temperatures of defects in tungsten created by self-implantation, Journal of Nuclear Materials 463 (2015) 329 – 332.

[22] H. Eleveld, A. van Veen, Void growth and thermal desorption of deuterium from voids in tungsten, Journal of Nuclear Materials 212 (1994) 1421 – 1425.

[23] T. Amino, K. Arakawa, H. Mori, Activation energy for long-range migration of self-interstitial atoms in tungsten obtained by direct measurement of radiation-induced point-defect clusters, Philosophical Magazine Letters 91 (2011) 86–96.

[24] L. Keys, J. Moteff, Neutron irradiation and defect recovery of tungsten, Journal of Nuclear Materials 34 (1970) 260 – 280.

[25] A. Debelle, M. Barthe, T. Sauvage, First temperature stage evolution of irradiation-induced defects in tungsten studied by positron annihilation spectroscopy, Journal of Nuclear Materials 376 (2008) 216 – 221.

[26] F. Ferroni, X. Yi, K. Arakawa, S. P. Fitzgerald, P. D. Edmondson, S. G. Roberts, High temperature annealing of ion irradiated tungsten, Acta Materialia 90 (2015) 380 – 393.

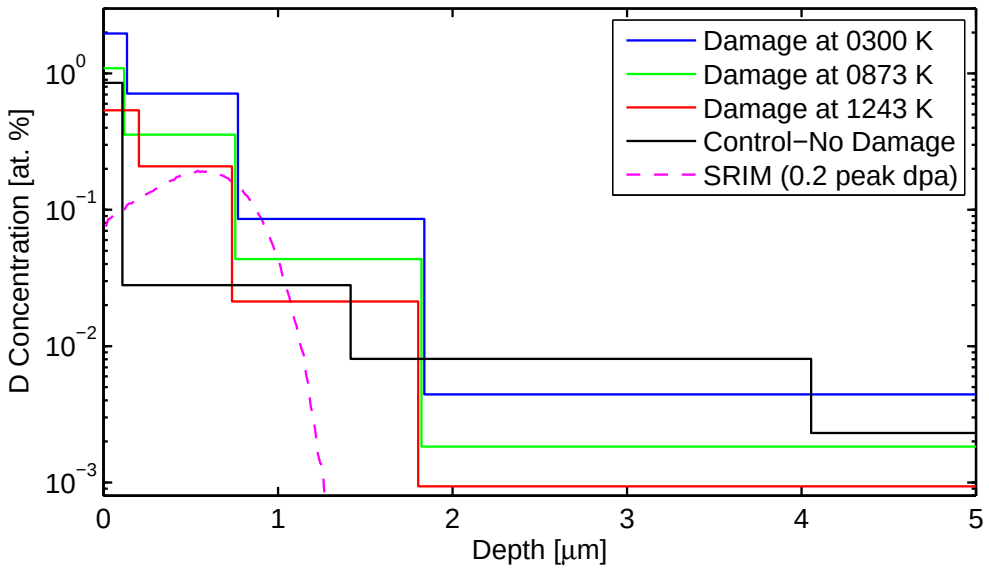

Figure 1: NRA measured D depth profiles for 3 samples of increasing temperature during displacement damage by 3.4 MeV Cu ions. The SRIM calculated dpa profile is also shown with a peak dpa of 0.2 near 0.6 μm.

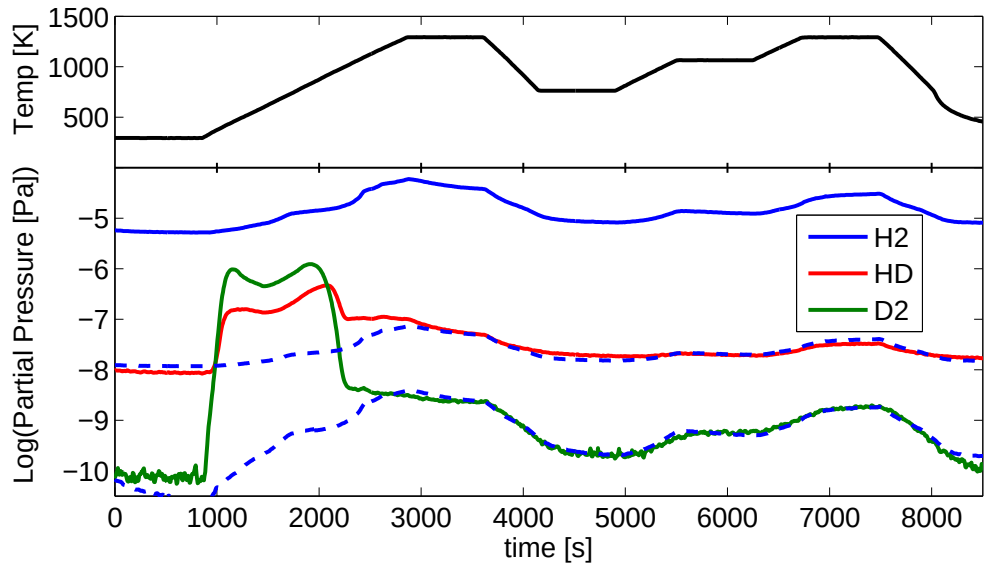

Figure 2: TDS data is shown for a sample with a linear heating ramp of 0.5 K/s held fixed at 1300 K and followed by additional cooling and heating ramps. Beyond the initial temperature ramp, the HD and D_2 has effectively degassed from the sample and what remains is primarily due to water on the chamber walls. Shown as blue dashed lines, the H_2 signal is linearly scaled to this background for HD and D_2.

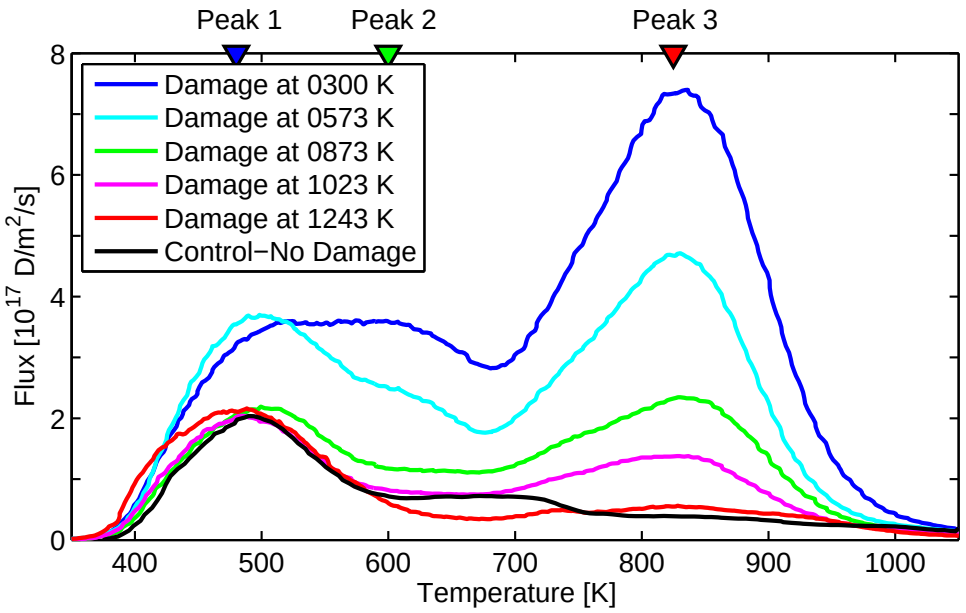

Figure 3: D release measured by TDS on samples simultaneously damaged with 3.4 MeV Cu ions while being heated. Decreasing retention trending toward the undamaged/control sample is found. Peaks 1-3 with release temperatures at 480, 600, and 825 K are indicated.

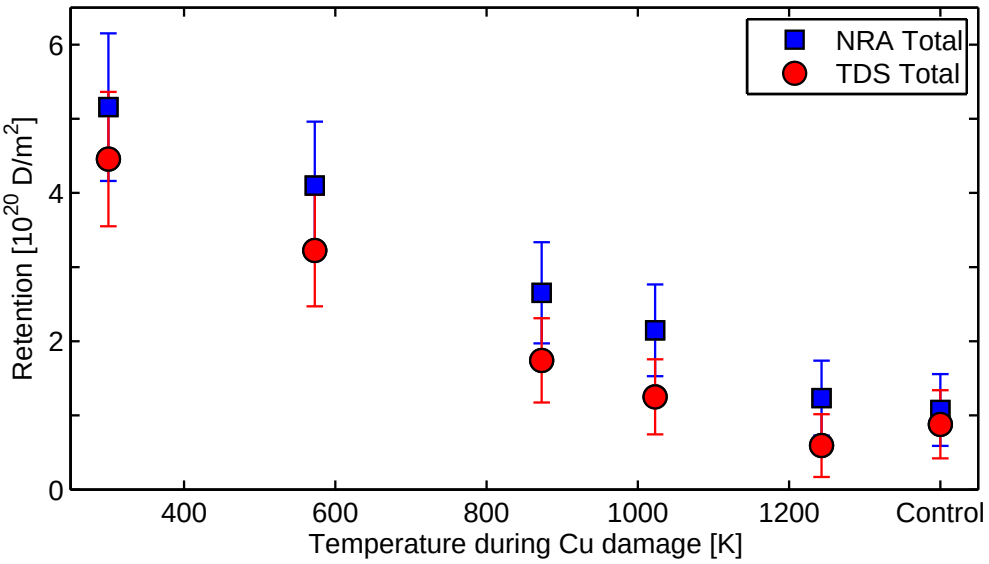

Figure 4: The total D retention measured via NRA up to 6 μm and TDS throughout the bulk of the samples.

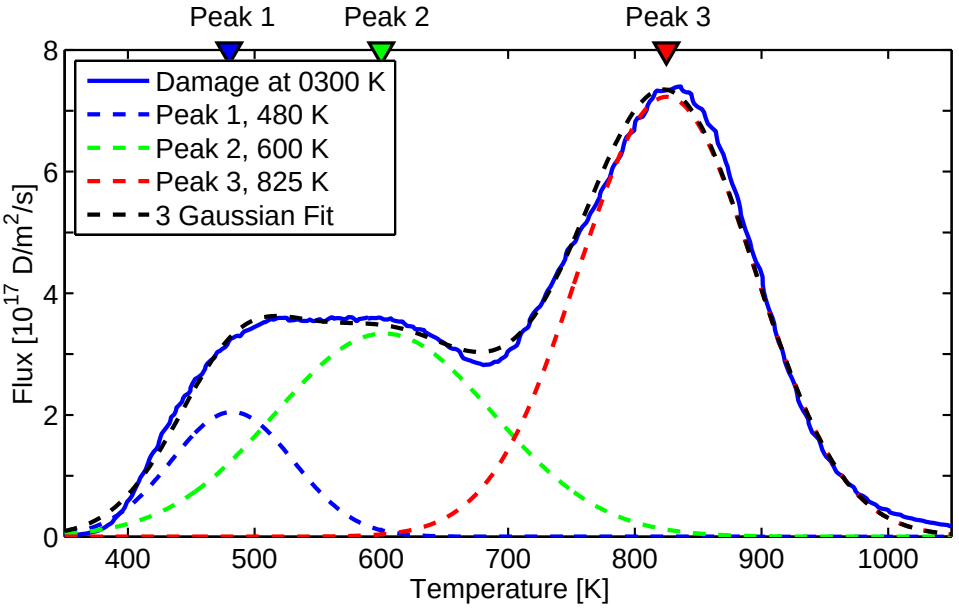

Figure 5: The thermal desorption flux (solid line) of D is fit with the sum of 3 Gaussians peaked at 480, 600, and 825 K (dashed lines).

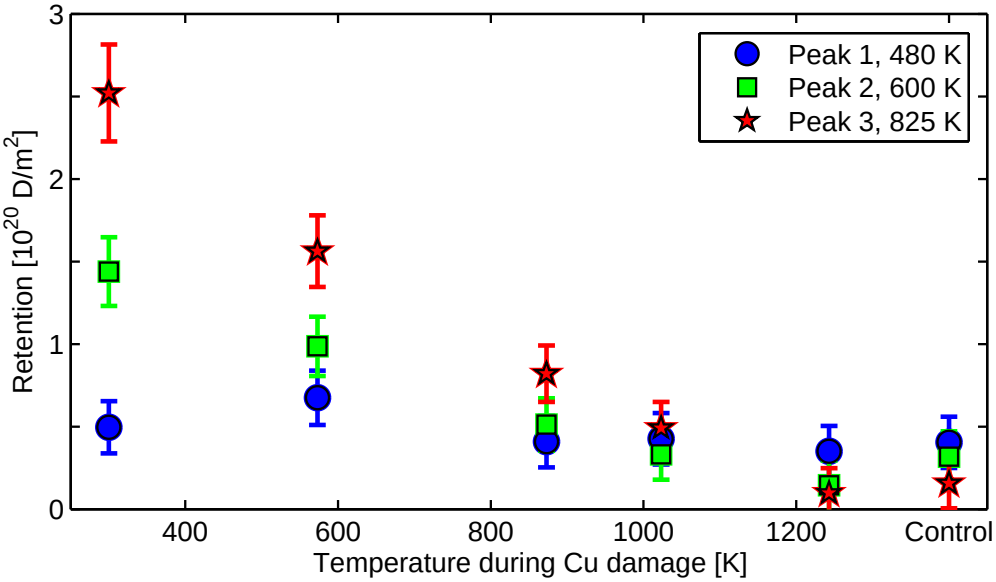

Figure 6: Three Gaussians peaked near ~480, 600, and 825 K were fit to TDS profiles of D release. The total D retention associated with each Gaussian is plotted here, demonstrating the recovery from damage with concurrent elevated sample temperatures.

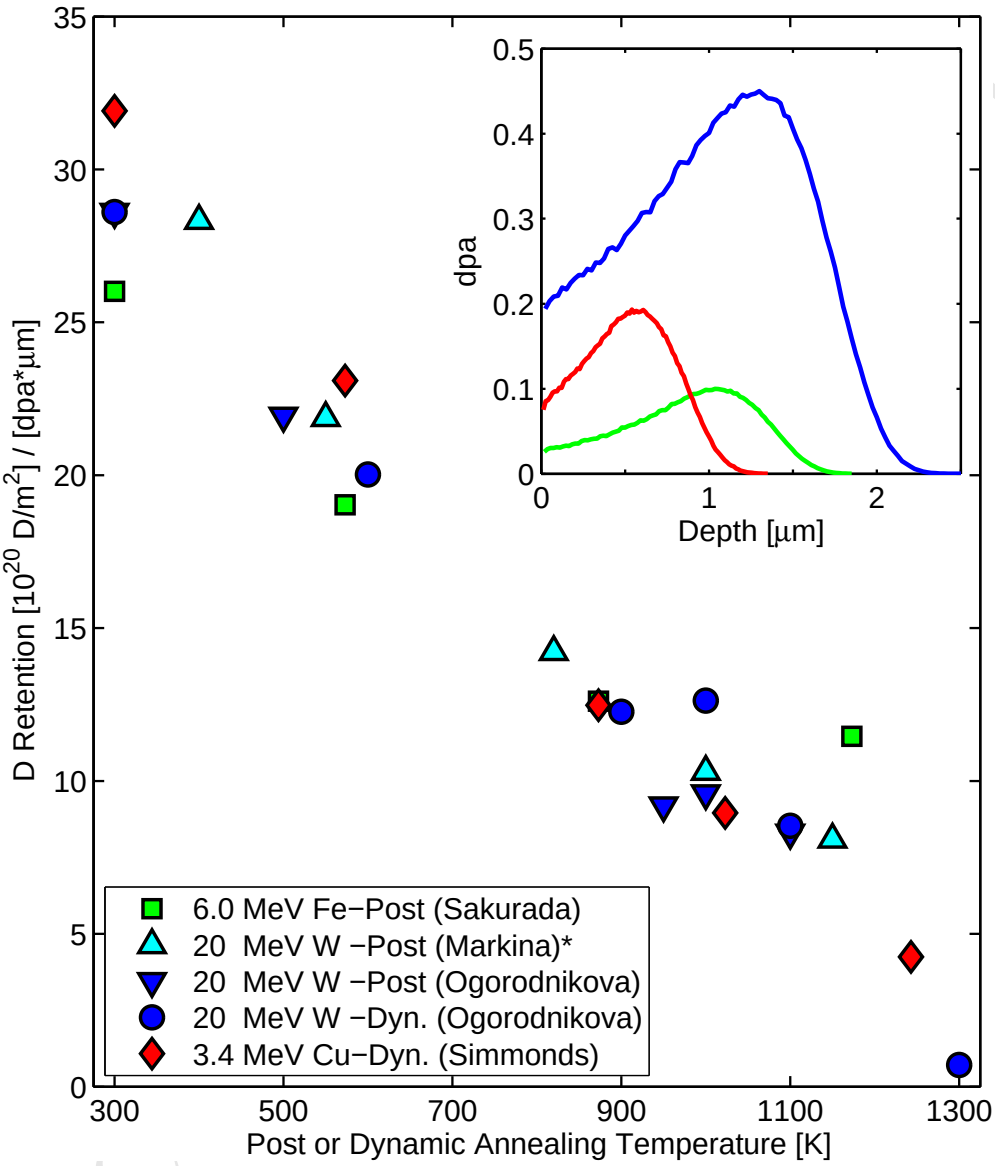

Figure 7: Total D retention normalized to the displacement damage profile (i.e. dpa*μm) shows agreement between Sakurada [7], Markina [21], Ogorodnikova [8], and this work. The inset plot shows the profiles for Fe (green), W (blue), and Cu (red) with peak dpa of 0.1, 0.2, and 0.45 respectively. *Note that Markina's peak dpa is scaled to 0.45.

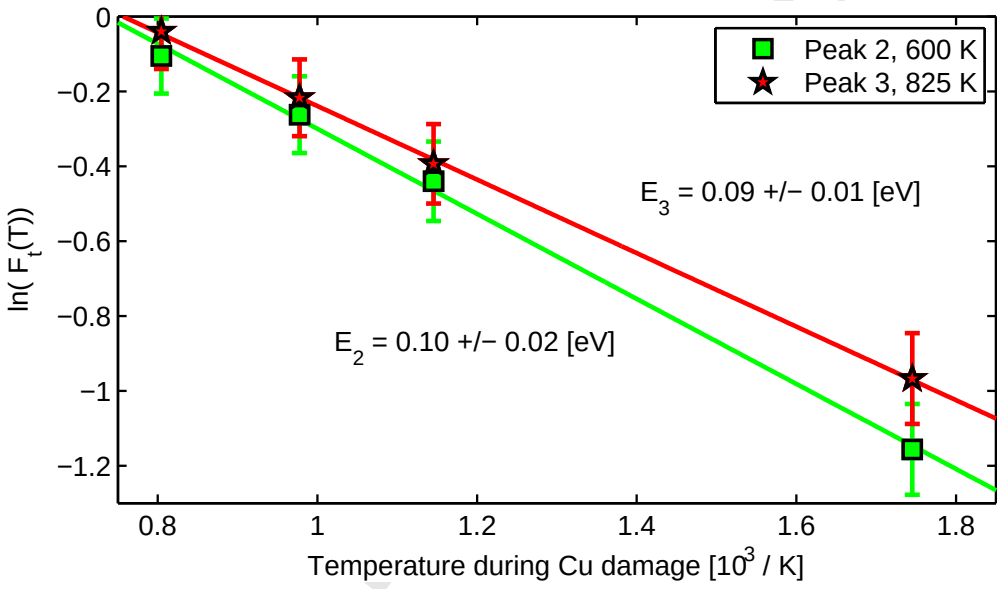

Figure 8: The fractional recovery, $F_t(T) = (R_t(300K) - R_t(T))/R_t(300K)$, for both high energy traps correlates with an activation energy of 0.1 eV.